ELSEVIER

International Journal of Mass Spectrometry 192 (1999) 347–365

International Journal of Mass Spectrometry

Photon observations on excited multiply charged ions

Elmar Träbert

Experimentalphysik III, Ruhr-Universität Bochum, D-44780 Bochum, Germany

Received 25 November 1998; accepted 17 February 1999

Abstract

Multiply charged ions are not only carriers of mass and charge, but have atomic structures of their own. These structures as well as the energy that may be stored electronically in such ions bear upon any processes that involve multiply charged ions. However, it is easier and the information cleaner when these properties are being studied at times when the ions are not undergoing collisions or interacting with external fields or with surfaces. The information is then regularly imparted by observing light that is from radiative processes. Techniques and results of such photon observations of multiply charged ions are presented. (Int J Mass Spectrom 192 (1999) 347–365) © 1999 Elsevier Science B.V.

Keywords: Multiply charged ions; Radiative processes; Atomic spectra; Atomic lifetimes

1. Introduction

The matter in the world around us is quasineutral, and positive charges (mostly of ions) and negative charges (mostly of electrons) balance. However, singly charged ions play important roles in biological and chemical processes. In principle, ions can be negatively charged (from additional electrons attached to the normal neutral state) or positively (when electrons are missing, usually due to some energetic mishandling of the atom). Theoretical and experimental evidence so far says that there are no multiply charged negative atomic ions. We will therefore deal only with positive ions, and will concentrate on those that are short of several electrons. In this deprived state, the Coulomb field reaches far and strong, so that multiply charged ions capture electrons in order to get closer to the neutral state, if electrons are available. Obviously such ions are more stable in a good vacuum, which is why they do not appear in nontechnical environments on Earth, with the possible exception of flashes of lightning. However, there are plenty of multicharged ions elsewhere, e.g. above the surface of the sun. There the vacuum is excellent; electrons are plenty and excite and ionize the atoms, but are too energetic to be readily captured by the ions. Collision processes certainly can produce multiply charged ions. However, we cannot put a particle detector close to the sun and check for the charge-to-mass ratios of particles out there. How do we then know what atoms are there that can be ionized and what charge states are being reached?

The first clues to the answers to this riddle are about 200 years old: Joseph Fraunhofer combined a telescope with a prism and found that the dispersed spectrum of the sun showed a number of dark lines on a more or less uniformly bright background. Half a century later, Bunsen and Kirchhoff discovered similar lines in the laboratory, the same wavelengths as bright lines (on a dark background) appeared when

1387-3806/99/$20.00 © 1999 Elsevier Science B.V. All rights reserved
PII S1387-3806(99)00076-7

burning certain materials in a flame. The specific wavelengths apparently were a signature of chemical elements and, depending on conditions, could be seen in emission or absorption. This not only initialized spectral analysis, but also furthered solar research: now it was obvious that the same species of atoms as on Earth occur in the sun. The same only? There were quite a number of lines, some of them prominent, that seemed to be observable only in the solar spectrum and not in the laboratory. Some lines were ascribed to an element that was believed to be present only in the sun ("helium"), until it was finally found on Earth, too. Other lines, notably from the solar corona (including the speculative element "coronium") that is visible only during solar eclipses, needed the best part of another century for their identification. In the 1930's, the development of the production and spectroscopy of multicharged ions was pushed by Edlén and Tyrén at Uppsala [1]. Then, in 1942, Edlén [2] showed that the small energy differences of spectral lines in the extreme ultraviolet [(EUV), transition energies of the order of 100 eV] that he had observed with ever more powerful electrical discharges (vacuum sparks) agreed precisely with the photon energies of various coronal lines (of order 2 eV). This proved the presence of highly charged ions of Ca and Fe (and later of many other elements as well) in the solar corona. The energies needed to ionize any atom to such a degree of ionization are in the range of a few hundred electron volts, but the visible solar "surface," the photosphere, is at a temperature of about 5500 K, or about 0.5 eV. This implication shook up the solar physics community, and it necessitated a complete rethinking of the structure of and the processes near the solar surface layers. When eventually hot plasmas were produced on Earth in the attempt to mimic solar fusion processes, spectroscopy was available to supply nonintrusive tools for plasma diagnostics. You cannot touch the sun, as it is so far away in space and gravitational potential, and you do not want to be near a hot fusion plasma. However, radiative processes take place and tell about the ions by the light: Catch the photons and learn about the emitter (and its surroundings)!

2. Ion production

Although singly charged ions can be produced in many processes (like thermal motion and collisions, field-emission, lower electric discharges, and others), further ionization is overwhelmingly achieved by electron–ion collisions of various circumstances. In the electron cyclotron resonance ion source (ECRIS), free electrons are heated resonantly by microwave radiation at a frequency determined by an external magnetic field. The energetic electrons then hit bound electrons of the atoms of the source gas and chuck them out of the atom. In the electron beam ion trap (EBIT) [3] or ion source (EBIS), the ions are confined and then exposed to a steady, intense stream of electrons, successively stripping away electrons from the ions. Before the advent of these ion sources, low charge state ions were accelerated and then passed through a gas or a thin foil [3–7]; by collisions mostly with the sea of target electrons, atoms would lose outer electrons and thus reach higher charge states. (There are many more electrons than atomic nuclei, and the energy transfer in binary collisions is more efficient among electrons than in collisions of atoms with electrons.) Although it was in this way that uranium was first stripped of all its electrons, at ion energies beyond 500 MeV/nucleon [8], it takes much more modest means to reach the same center-of-mass collision energy (and thus reaches the same ion charge state) by 250 keV electron bombardment of U ions trapped in an EBIT [9]. However, there are factors and physics problems involved, in particular the inherent time resolution at the few picosecond level, that necessitate the use of the high-energy accelerator for some atomic physics applications. The fraction of ions not in their atomic ground state differs from one type of ion source to the other and also depends on the operating conditions and on the ion energy. Literature values vary from a few percent to some 50%. Depending on the lifetimes of the levels involved, this may mean a very notable or a negligible effect for the user of the multiply charged ions. Collision cross sections of excited ions are certainly larger than those of ground state ions, in some cases by orders of magnitude, so that even a small fraction of excited

ions may need to be taken into account in quantitative experiments.

3. Structure and dynamics

The analysis of spectra like those observed by Bunsen and Kirchhoff, combined with the concept of the atom consisting of a nucleus and electrons, led to conclusions as implied by Bohr's postulates: The atom has specific energy states; any energy absorbed or emitted matches the energy difference of initial and final states. Additional reasoning about angular momentum and quantization (Planck's constant h) and incorporating the empirical Balmer formula would then yield proper estimates of the energy states of a simple atom, like hydrogen. Unexplained at the time remained other, also very basic observations: Most elements have much more complicated spectra (later identified as multielectron spectra, with electron–electron interactions and particular coupling systematics), and spectra had much fewer lines (and of very different intensities) than could be assumed if any combination of levels could result in an atomic transition (additional quantum numbers, selection rules, transition probabilities). Quantum mechanics would be needed to deal with all these aspects of atomic structure and dynamics, and then the need to include relativity would show, and quantum electrodynamics as the first successful quantum field theory would follow.

With the 92 elements up to uranium and all their ionization stages, there are of order 4000 atomic systems, each with its own characteristic spectrum. Leaving out neutral atoms and ions in low charge states, the number of different multiply charged ions is still far beyond 3000. What is needed is some kind of systematization to structure this multitude and get a handle on the physics. Electrons fill up atomic shells obeying the Pauli exclusion principle. Adding an electron changes the number of electron combinations and the total spin. Therefore the concept of elements (the number of protons in the nucleus) is of very limited use with multiply charged ions. On the other hand, the atomic structure (dominated by the number of electrons) is rather similar with all ions that have one (two, three, or more) electrons. The common parameter in such isoelectronic sequences is the number of electrons; the running parameter, incrementing by integers, is the nuclear charge. Such sequences are then named after the element at the neutral end of the sequence, be it H, He, Li, or whatever else. Hylleraas [10] found out that many atomic parameters (such as level energies and their differences, line strengths, oscillator strengths, transition probabilities, etc.) could be described by series expansions with characteristic leading terms. Again, Edlén [11] provided practical recipes for the application of these ideas to experimental data. There are deviations from the simple trends for ions of low charge state and for neutrals, but those are anyway of no interest in the present context (for a tutorial on the basics, see [12]). We therefore enjoy the benefits of isoelectronic comparison and scaling: If characteristic properties of a few cases in an isoelectronic sequence have been determined by experiment or calculation, it is fairly straightforward to obtain valid estimates for other ions in the same sequence that have not been covered before.

One has to keep in mind that different atomic properties may scale differently with the nuclear charge Z (or the ion core charge $\zeta = Z - N + 1$ that the valence electron experiences, with N being the number of electrons, and possibly a screening correction), and thus some properties may be unimportant in comparison to others or be dominant in different parts of an isoelectronic sequence. For example, the energy difference between atomic shells with quantum numbers n ($\Delta n > 0$) scales with Z^2 as in any H-like system (see the Bohr formula). The fine structure splitting, a relativistic effect, scales with Z^4, as does (approximately) the Lamb shift, a quantum electrodynamic (QED) effect. Consequently the fine structure splitting increases toward uranium on a relative scale, but remains in proportion with the QED contribution. However, if the ion has several electrons, the degeneracy of levels of a given principal quantum number n is lifted, and electron–electron interaction introduces level splittings (and $\Delta n = 0$ transitions) that increase linearly with Z. Compared to these, the Z^4

dependence of the relativistic effects can be quite massive, with drastic changes of the level structure for high nuclear charges.

Transition probabilities also show interesting Z dependences. The basic electric–dipole (E1) $\Delta n > 0$ transitions as described by the Bohr formula scale with Z^4. This means that nanosecond lifetimes in H correspond to sub-picosecond lifetimes in Ne^{9+} and beyond, and such short lifetimes probably are measurable only by observing natural line widths—a formidable challenge in most situations. However, the probabilities for E1 transitions within a given shell ($\Delta n = 0$) scale linearly with Z and thus remain measurable even in very highly charged ions [13–15]. There also are levels that cannot decay by E1 radiation because there is no lower level of opposite parity. Such levels often can decay by magnetic dipole (M1) or electric quadrupole (E2) radiation, which is of negligible probability at low Z, but scales with Z^{10} and Z^8, respectively, often becoming dominant at high Z. Last, but not least, there are E1 decays that are hindered by the spin-conservation rule that defines LS coupling (L is the sum of the angular momenta, S is the total spin, both are then coupling to a total angular momentum quantum number J). These transitions connect levels in term systems of different level multiplicity (different spin) and therefore are called intercombination lines. The transition probability may scale as steeply as Z^{10} for low Z and $\Delta n > 0$) or be close to Z^7 (for $\Delta n = 0$) (individual electron angular momentum l and spin s couple to total angular momentum j; then these individual j values couple to yield J) (see examples discussed in [16,17]). With *jj* coupling being approximated for high Z, the concept of multiplicity and intercombination transitions fades, but even in *jj* coupling the corresponding level remains relatively long lived. What is interesting in these cases is that higher-order terms in atomic structure become observable and even measurable, when the normal, lowest-multipole order transitions are blocked. Lifetime measurements then sense these higher-order terms directly. An extreme case (no lifetime measurement yet) is the observation of a magnetic octupole (M3) transition in Th^{62+} and U^{64+} [18].

4. Light sources

Atomic structure and dynamics are intertwined. The different energy ranges and time ranges require a variety of detection systems and schemes. However, there are light sources that yield information mostly on structure, and others that yield better access at the dynamics in the ion. For time-integrated observation, we might, for example, look for light right inside the plasma. What we normally find there is some steady-state situation, a dynamic balance of excitation and de-excitation processes. Although that may be typical for a working plasma, it is not ideal for obtaining information on individual ionic species, except for monitoring and perhaps optimizing their production. The observation of other plasmas will suffer similar setbacks, but specific plasmas may nevertheless offer specific properties that are valuable for spectroscopy.

An example is the aforementioned solar corona. It is hot and thus contains heavy ions (mostly up to Fe) in many charge states; in solar flares, even Fe can be fully ionized. This comes about by a steady supply of fast electrons and protons (solar wind) for excitation and ionization, but at an electron density that is so low that there is little (but some) chance for recombination with ambient electrons. The typical time intervals between collisions are much longer than even the very long (microsecond, millisecond) lifetimes of particular levels in some highly charged ions, which gives them the chance to de-excite by emission of light. The solar corona does vary in its properties, but the changes take place on the scale of minutes, hours, and days. From a spacecraft in Earth orbit (much of the spectrum is blocked by the atmosphere from reaching observers on the ground), extended exposure times are possible, permitting very high spectral resolution work. The result are spectra of high quality. However, there are many elements in the sun, and laboratory work is necessary to find out what line belongs to what element. Also, in order to interpret the observations for the understanding of coronal conditions, additional information on collision processes and radiative decay rates has to be obtained from theory and laboratory work [19,20].

The sun's inner workings are nowadays assumed

to be fueled by nuclear fusion. Among the terrestrial devices that seek to emulate this energy conversion is the tokamak, a ring-shaped plasma discharge with confining magnetic fields. The plasma in the tokamak is much denser than the solar corona, but by terrestrial standards it is still a low-density plasma. Because of this low density, tokamaks need to reach temperatures much higher than those of the interior of the sun, and therefore as a spectroscopic light source they are more related to the corona. The higher densities than in the corona imply faster collisional quenching, so that levels with lifetimes exceeding, say, 1 μs are suffering from this. In terms of highly charged atoms, tokamaks have provided data on ions like almost bare Fe and Ne-like Eu^{53+} [21–26]. Tokamaks have developed from millisecond pulse lengths to second-long pulses. However, on an atomic scale, for practical purposes this range still means a steady state that yields little information on atomic dynamics.

Higher charge states (up to $q = 53+$ for Na-like ions [26–32]) have been reached in dense plasmas that were produced by tight focusing of laser light onto the surface of a solid. Using nanosecond pulses at power densities of TW/cm^2, the material in the laser focus is converted quickly into a plasma plume that becomes opaque to further irradiation and then that expands into vacuum. The high electric field strength of the intense laser light produces very fast electrons that rapidly ionize the atoms in the plasma until densities drop off from the expansion. This is a highly transient phenomenon, but by clever observational tricks one can deal with some factors that limit the spectroscopic exploitation. For example, observation is being done parallel to the surface and at a distance of about 1 mm from it; this avoids the hottest and brightest part of the plasma in favour of a region where the plasma mostly streams away from the surface, and is viewed at right angles which minimizes the Doppler effect of the fast ion motion. Furthermore, a line-shaped focus (that is observed along its length) optimizes the ratio of ions moving in parallel to those expanding rim sections. The density of the plasma that is advantageous for reaching high charge states quickly is, however, adverse to the wish of observing long-lived ions. Dense, laser-produced plasmas, remarkably, are themselves media that may show amplified stimulated emission (ASE), a major step toward real lasers in the EUV or soft-x-ray range. For a glimpse of what has been reached within the first decade of ASE in the soft-x-ray range, see [33].

Time-resolved observation of atoms or singly charged ions has for a long time been effected by (pulsed) electron–atom collisions and then by pulsed lasers, or lately by fast atomic beams and continuous wave (cw) lasers. However, we want to discuss multiply charged ions, and their production and observation, in particular, by time-resolved measurements; this is a complex matter. For meaningful time-resolved observations on multiply charged ions, light sources with completely different concepts are needed. Of these we will discuss foil-excited fast ion beams and traps of different designs (electrostatic trap, storage ring, electron beam ion trap) and evaluate their respective merits.

5. Foil-excited ion beams

When a beam of fast ions (in a vacuum) is being passed through a thin foil, not only a charge state distribution among the emerging ions is found, but also light can be observed: The interaction of the projectile nucleus and electrons with the target electrons is so violent that multiple excitation occurs with subsequent autoionization, and there also can be electron capture upon leaving the foil. The ions are much heavier than the electrons they collided with, so that the ions continue with only little change of speed and direction. (Nuclear collisions would result in larger deflections.) The ions travel with constant velocity in a high vacuum (no external perturbations), so one can observe their electronic restructuring. The flight distance behind the foil immediately corresponds to the time-of-flight since the last massive perturbation. Tracking a spectral line as a function of distance yields a decay curve that can be evaluated in terms of atomic lifetimes in the few-picosecond to many-nanosecond range. Observing spectra at different locations along the ion beam yields spectra that are prompt or delayed, and therefore are dominated by

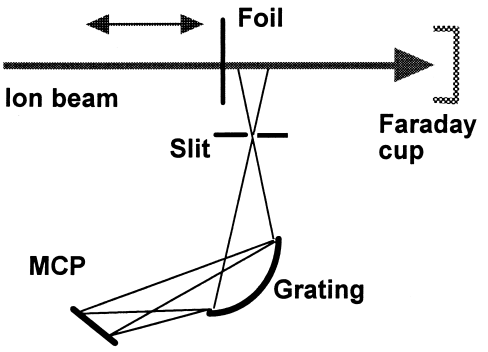

Fig. 1. Schematics of beam–foil spectroscopy: A well-collimated beam of fast ions traverses a thin foil and continues with almost the original velocity. Observation of a section of the excited ion beam is intrinsically time-resolved. Here a grating spectrometer with a microchannelplate (MCP) multichannel detector is sketched.

the decays of very short-lived or of longer-lived levels. The acceleration and ion transport system combine in providing an ion beam of isotopic purity, on which intrinsically time-resolved (by sheer geometry) observations in the subnanosecond range are possible. (See Fig. 1.)

The technique has been realized by Kay [4] and Bashkin and co-workers [5,6] around 1963. It has since expanded to some of the largest accelerators, work has been done on states up to the highest charge of the heaviest element [13,14]. Beam-foil spectroscopy has been put to very many uses, from fundamental wavelength and lifetime spectroscopy on few-electron systems [34–40] to the provision of comparison spectra for plasma devices or the elemental identification of lines in the solar corona [41].

However, there are problems [7]: The excitation by ion–foil interaction is nonselective. This has the advantage of reaching excited levels that are not reached in other light sources, like many multiply excited systems with several electrons not in their lowest states. (For experiments on processes this implies that very much excitation energy can be transported in an ion, by distributing the energy to several electrons.) This also has the disadvantage that the spectra are very rich in the number of lines, but not in their intensity, so that line blends are frequent. The low light intensity necessitates the use of poorer spectral resolution than is available with other light sources (although some of that can sometimes be saved by the technique of refocusing [42,43]); wider spectrometer slits or larger detectors result in Doppler broadening. For wavelengths there is also the problem of Doppler shifts, for lifetime measurements that of cascade repopulation. Ingenious techniques can sometimes work around these problems so that precise wavelength and lifetime measurements are possible. This is important, because there are cases where beam–foil spectroscopy is the only tool available. Such is the case for the systematic study of the transition probabilities of resonance and intercombination transitions in few-electron systems (Li, Be, Na sequences [15,44,45]), or delayed spectra that illuminate the role of very long-lived excited levels in highly charged ions [34], or for differential lifetime measurements that are sensitive to higher-order autoionization effects [46] or to hyperfine structure [47,48].

There are many successes of beam–foil spectroscopy, but as a physicist one is interested in preparing the systems of interest in the cleanest possible way, and for such goals new tools have been developed recently.

6. ECRIS, EBIS, EBIT

Beams of fast ions can be further ionized by being passed through thin layers (foils or gases) of matter, and in a multistep process with several stripping stages, accelerators can reach very high ion energies and very high ion charge states. In order to save some of the steps, ion sources have been developed that permit an accelerator to start out with multiply charged, if not highly charged ions, instead of the singly charged ions used for decades. One of these ion sources is the aforementioned (ECRIS), which uses a plasma inside a strong magnetic field. Free electrons gyrate around the magnetic field lines, and this motion can be sped up by sending in microwave radiation at the cyclotron resonance frequency. With sufficient microwave power and an appropriate source geometry, high charge states can be reached, and ions of Xe

can be almost fully stripped. ECRIS is an interesting ion source, but it has only limited value for a light source to be studied spectroscopically. However, ions extracted from ECRIS at kiloelectron volt energies may be guided to gas targets. Photon spectroscopy (of the ions that have captured one or more electrons in the collision) then reveals that ion–atom collisions in this energy range often lead to peculiarities of atomic level populations and thus to interesting insights into the collision process (for a small, nonrepresentative selection of the many studies, see [49–56]). The ion currents apparently are not yet high enough to permit high resolution spectroscopy, though.

An alternative design is the EBIS. It basically is a Penning trap with a strong magnetic field. An intense electron beam is injected along and thus guided by the magnetic field. If inside the trap volume [defined by the magnetic field (for radial confinement) and by charged electrodes (for axial confinement)] an atom is ionized by the impinging electron, it is immediately trapped. The ion cannot move out, but may be hit by more electrons which successively strip off further electrons from the trapped ion, increasing its charge state. The radial trapping of ions is aided by the space charge of the electron beam (however, the ion cloud expands, but remains trapped when the electron beam is switched off, as is being done in atomic lifetime measurements). Ambient slow electrons may be captured. The balance of ionization and recombination depends on the available electron energy and the ionization energies of the ions in the respective charge states. The ionization limit is reached when the next ionization step would require more energy than is available in the electron beam. There also are some ion losses due to recombination with ambient electrons, or charge-changing collisions with rest gas atoms that may result in drastic changes of individual ion trajectories. The ionization process works best with a good spatial overlap of the electron beam and the accumulating ion cloud; this overlap is aided by the space-charge compensation that the electron beam provides for the ion cloud until the space-charge limit is reached, the electron beam even provides an attractive potential. With the electron beam around, ionization and recombination are possible and contribute to a dynamic balance that depends on the electron beam density and energy. After a while (up to a few seconds for the highest charge states), a steady-state equilibrium is reached, with a certain charge state distribution. As the electron beam energy can be adjusted, any charge state of any element can be reached and studied—with spectroscopic precision [57–63].

EBIT is a very stable and rather clean light source. The ion cloud is about 2 cm long and has a diameter very much like a human hair, about 70 μm. In order to maintain optimum light collection, this well-defined radiating cloud can be observed immediately, without an extra spectrometer entrance slit. Practical operation of this light source, however, is a bit more complicated: Ion trapping is aided by bleeding in light-atom gases, like nitrogen, and there always are heavy-ion contaminants like Ba (from the electron gun) that tend to accumulate in the trap volume and need to be purged regularly.

7. Level lifetimes

Line strengths, transition moments, oscillator strengths, and level lifetimes all (largely interchangeably) describe how an atom or ion responds to electromagnetic fields: To real fields by absorption or stimulated emission, or to the so-called vacuum fluctuations by spontaneous emission. Some transitions seem easy and correspond to bright lines and high transition probabilities, others are possible, but less likely (lower transition probabilities) and often found to violate some conservation rule (spin or else). Yet other lines that would correspond to a level difference in the atom do not occur at all. These cases are described by selection rules that link the properties of the electromagnetic field and the symmetries of the atomic system. We call allowed transitions those that imply electric dipole radiation (E1) and connect levels of opposite parity; this implies also that the total angular momenta J of initial and final states must not differ by more than one unit, nor must both be equal to zero. Corresponding rules can be formulated for the next terms in a multipole expansion of the radiation field. We will discuss some of these in our examples.

Right now we only need to realize that the transition rates for different types of transition can be very different and scale differently with the nuclear charge *Z*. The different time ranges, just as the different energy ranges, require different technical measures for detection and proper measurement. We concentrate on cases of multiply charged ions. This excludes, for example, absorption measurements, as the density of multiply charged ions is rarely high enough to render absorption of radiation measurable. The following discussion roughly moves from femtosecond lifetimes to the second range.

In EBIT, the kinetic energy of the trapped ions is limited by the axial electrode potentials (usually a few hundred volts); ions that are too fast leave the trap. High-resolution spectroscopy shows that emission lines from excited ions are Doppler broadened because of the kinetic energy of the ions. By lowering the potential barriers, the faster ("hotter") ions escape, and the "temperature" of the remaining ion cloud is being reduced (as is seen by the reduced Doppler broadening). Usually some light element gas (nitrogen) is bled into EBIT to provide a "collisional coolant" for the heavier ions of interest. In some cases the cooling extends far enough to let the natural lifetime broadening of extremely short-lived atomic levels become visible. Lifetimes in the femtosecond range can then be determined from a measurement of the line width, as has been demonstrated by high-resolution x-ray spectroscopy on Cs^{45+} ions trapped in EBIT [64].

With traditional beam–foil spectroscopy and ion energies of order 0.5 MeV/nucleon, the ion velocity is 1 cm/ns. If the optical detection system or the mechanical foil drive is capable of micrometer precision displacement, picosecond lifetimes are measurable, in favourable cases even subpicosecond lifetimes. On the long lifetime side, a vacuum chamber will normally not be longer than 1 m (or 100 ns time of flight); using the beam pipe for an extension, we get up to a few hundred nanoseconds, but we get also into trouble because of ion beam geometry (divergence), optical field-of-view and so on. Thus the optimum working range of beam–foil lifetime measurements is from picoseconds to, say, 30 ns. If a level has a lifetime not very different from those that decay into it (decay chains or cascades), the decay curves are difficult to analyse and may suffer badly from systematic error. However, by observing such cascades directly and performing a correlated analysis, the lifetime precision can be as good as about 1% in very favourable cases, though 3 to 10% is more typical. This is as good or better than most calculations. Only on few-electron systems, for example the resonance lines in Li- and Na-like ions, there are battles being fought for higher precision in theory or experiment, and the advantage has been on either side at given times. For some systems now theory seems to be in the lead, but not for ions with more than one electron in the valence shell.

For much longer atomic lifetimes than 30 ns, different techniques are needed. Even slowing the ion beam down, by the way, does not help that much: Reducing the energy by a factor of 100 reduces the velocity (and thus the geometric time scale) by a factor of 10 only—and already necessitates a decoupling of the charge state production (which with beam–foil experiments is happening in the foil or a gas target) from the ion energy [65,66]. A dedicated ion source (ECR or EBIS, as mentioned above) might go some way, but not very far, as their output beams are either not well collimated or not very intense (for a general discussion, see [7]). The only way out, apparently, is the trapping of such ions.

In conventional ion traps, the energies of the stored particles are less than, say, 100 eV. Penning [67], Radiofrequency (Paul and Steinwedel [68] and electrostatic (Kingdon [69]) [70–72] ion traps have been used for lifetime measurements of a fair number of intercombination and some forbidden transitions in low charge state ions. The lifetime range covered is about 0.1 ms to a few seconds, with typical uncertainties of the results near 5%, although earlier measurements sometimes scattered by much more. Much of this uncertainty is due to charge exchange collisions. Working at low pressures to keep collision rates low also implies a weak signal, because there is so little material to produce ions from, unless one produces the ions elsewhere and transfers them into the trap, or from one trap to another one that operates under

cleaner conditions. In order to find the true lifetime, one does measurements at various pressures and extrapolates the measured lifetimes toward zero pressure. Some of such lifetime measurements have reported data at the 1% level of uncertainty.

8. Storage ring—an endless trap for high-energy particles

The cross sections for charge-changing collisions are large in the energy range of less than 100 eV where most of the above light sources and traps operate, but much smaller for more energetic particles (beyond the Bohr velocity, that is beyond 25 keV/u). However, beams of energetic particles are traveling too far within an atomic lifetime to permit reliable lifetime measurement in the range above a few microseconds when using standard beam–foil techniques. A way out of this dilemma is to take a fast ion beam and curve it back on itself, forming a ring. In such a storage ring, the ion beam can travel for thousands or millions of kilometers (and does), if the vacuum is good enough. Instead of moving a target or a detector, the ring is being filled once, and then the observer can sit still and watch the ion beam decrease in current (inevitably, because the vacuum will not be perfect) and record some signal from the given long-lived excited level of interest. Typical heavy-ion storage rings have circumferences of order 30–100 m, and the ion beams take 2–10 μs per turn. If one wants to follow the signal for a few turns of the ion beam, this implies a lower lifetime limit of order 100 μs; the upper limit results from collisions that change charge state and trajectory. For low charge state ions of a few megaelectron volts energy, this storage time may be a few seconds, and for high-charge state energetic beams (100 MeV/nucleon), this can well be many hours or days. The optical signal from the remaining ions has to be corrected for the number of the remaining ions, but this is simply done by a continuous measurement of the stored ion current. The lifetime of ions stored in a storage ring is much larger than that in radiofrequency or Kingdon traps for several reasons: In order to optimize storage times, the vacuum of storage ring vessels needs to be extremely good (10^{-11} mbar and better). This is possible, because the ion beam to be stored is produced elsewhere and only then injected into the ring, whereas with classical ion traps the ions often are produced inside the trap—necessarily at a worse pressure. Also, the collisional cross sections for a variety of processes are large at low (electron volt) collision energies which are typical for classical ion traps; storage rings, however, operate on megaelectron volt ions that by virtue of the high collision energies feature collision cross sections are lower by several orders of magnitude.

Heavy-ion storage rings have been built at Heidelberg (TSR), Aarhus (ASTRID), GSI Darmstadt (ESR), Uppsala (CELSIUS, a former part of a chain of accelerators at CERN), and Stockholm (CRYRING). All of these accept ion beams from an accelerator and can then work as a circular accelerator to boost the energy of the stored ions, and all of them have devices to reduce the momentum spread of the ion beam (“cooling”). (For enlightening conference proceedings and survey papers, see [73–77].) The most common device is an electron cooler, where a beam of electrons travels with the ions for a section of a meter or so and is then deflected away again. These electrons are produced as a “cold” beam, by controlling the emission process from the source, kinematic compression, and adiabatic cooling, and they are adjusted to travel at the same velocity as the ions in the storage ring. By collisions with the ion beam, the “thermal” energy of the ion beam gets distributed over ions and electrons, that is, the ions lose some momentum spread, and the electrons are burdened with some. The electron beam is deflected out, and the ion beam, now “cooler” than before, proceeds (Fig. 2).

9. Spectroscopy on one-, two-, three-, and four-electron systems

The spectroscopic tasks on multiply charged ions can be sorted by the growing complexity of atomic systems, from one- to many-electron systems, from gross structure via fine and hyperfine structure to

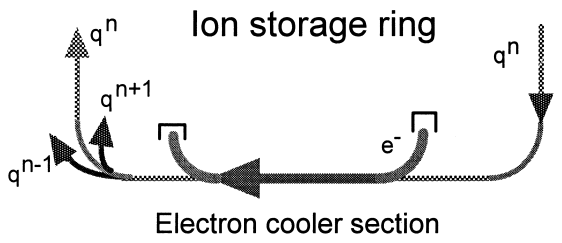

Fig. 2. Schematics of an ion storage ring section with an electron cooler. Ions that change charge state by interaction with the merged electron beam leave the storage trajectory at the next bend of the ring and can be detected.

QED effects. Connected with these are (electric–dipole) allowed and (electric–dipole) forbidden transitions, intercombination decays, higher-order multipole radiation and hyperfine-interaction induced decays. There are multiphoton decays and interference effects that become apparent in emission patterns. Obviously, complete coverage would exceed the scope of this manuscript, and only a few samples can be presented.

One-electron systems are the ones that have been calculated to the highest precision, and largely more precise than can be measured in ions beyond hydrogen (which can be studied by extremely precise laser techniques). If a system can be calculated so well, it is small effects that are of interest and want to be measured against a "background" of large contributions. Among these small effects are QED and hyperfine structure effects. QED effects are often labeled as the Lamb shift, which in turn is dominated by the self-energy contribution—most other QED effects largely cancel each other [78]. Although there have been a number of experiments on the $n = 1$ and $n = 2$ Lamb shifts (the deviation of the $1s_{1/2}$ level energy from the value predicted by Dirac's relativistic calculation, and the level shift of the $2s_{1/2}$ level from the Dirac energy of the $2p_{1/2}$ level), presently, in high-Z atoms theory seems ahead in precision. Lamb shift measurements in multiply charged one-electron ions have been tried in many ways, from the optical analog of the classical Lamb and Retherford experiment, trying to induce the $2s$–$2p$ transition by laser light [79] over attempts at mixing states of different parity by external fields [80,81] to spectroscopic observations of various kinds. (For a survey of the pre-EBIT and pre-storage ring Lamb shift experiments on multiply charged heavy ions, see [82].)

The short lifetime of the $2p$ levels results in a level width that is about one tenth of the mean transition energy. For very heavy ions, this transition energy corresponds to wavelengths in the visible–ultraviolet (VUV) and EUV spectral ranges, where spectrometers and detectors are not very efficient. It then seems better to observe the ground state transition $1s$–$2p$, which involves a large amount of less interesting hydrogenic transition energy, but also the eight times larger ground state Lamb shift (the Lamb shift scales with n^{-3}, n being the principal quantum number). Obviously, such a measurement in the x-ray range needs to be very precise to yield a meaningful number on the QED part, and several decades of development were needed to bring about very high precision. One major problem that turned up was the lack of precise reference wavelengths, which needed much thought and insight to overcome. The regular procedure requires the careful measurement of reference data in a standards laboratory and the development of portable references in the form of transfer light sources, whose reproducibility requires a lot of attention. Nowadays there is a second option, that is, x-ray diffraction crystals can be characterized in terms of optical interferometrical standards [83]. A pertinent problem is that of which light source to exploit for the actual measurement. Tokamaks, laser-produced plasmas, foil-excited fast ion beams were all tried. At present the best contenders are EBIT and heavy-ion storage rings with an electron cooler. EBIT is a stationary light source and thus has few problems beyond the intricacies of precision x-ray spectroscopy itself. The competitor technique has a few more problems, in particular the Doppler shift, and therefore it has not quite achieved the same accuracy, but is interesting in its own right and deserves a discussion.

If a fast ion beam is observed at right angles, the first order Doppler shift is zero, but the Doppler broadening (due to a finite solid angle of observation) is at a maximum. Along the ion beam trajectory (forward or backward), the shift is at a maximum, but

the broadening would be minimal. With a storage ring, the latter geometry is feasible, by putting the detector at the next bending magnet, so that the ion beam is deflected away before it would hit the detector. Excitation of the level of interest is achieved by electron capture in the electron cooler, with almost no momentum transfer. Ions that capture an electron move on a separate trajectory afterwards and can be detected with practically 100% efficiency. Thus x-ray detection can be done in coincidence with the capture event, and very clean spectra can be obtained [84,85]. The systematic error problems lie in the geometric setting and the need to establish the ion velocity with high precision.

Both experimental techniques, using EBIT or storage ring, are presently near 10 eV uncertainty for the ground state Lamb shift in U^{91+} (or few-electron ions of U). This is terrific, but theory claims that the uncertainty level of the calculations is down to 1 eV or less, and an experiment testing theory would need to do better than that.

In contrast, there is another case of a one-electron heavy ion system where experiment leads theory by a wide margin: The 21 cm line of atomic hydrogen, a mainstay of radioastronomy, originates from the transition between the two hyperfine structure levels of the ground state. The energy of such transitions scales with Z^3, and for $^{209}Bi^{81+}$ the line is in the near UV (243 nm). It has been observed—after a lengthy search—at the electron storage ring (ESR) at GSI Darmstadt [86]. A Doppler-shifted laser pulse was used to excite the upper hyperfine level from the lower one, and the subsequent fluorescence was observed. One feat was the finding of the resonance, but another interesting entity is the atomic lifetime measured on this transition. Even after detailed calculations and modeling of the magnetic moment distribution in the nucleus, theory is not yet in agreement with the experimental finding of 0.35 ms—off by about 15%. The same transition has been seen in EBIT, in isotopes of Ho ($Z = 67$) or Re ($Z = 75$) [61,63], where precise wavelength measurements are much easier to achieve, without need for a laser, by straightforward spectroscopic observation. Again, theory does not match the experimental findings yet.

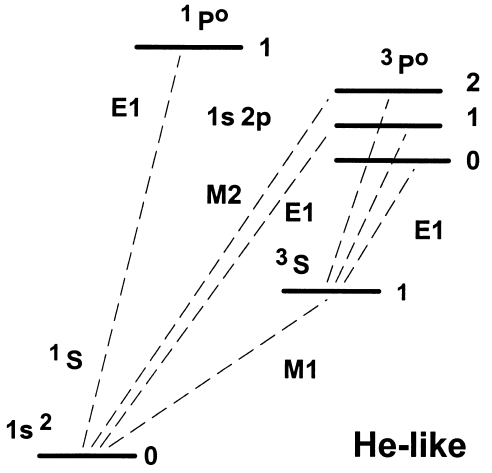

Fig. 3. The strongest transitions in a simplified level scheme ($n = 2$ only) of a two-electron ion. (The energy intervals are not to scale.)

10. He-like ions

In the multiply charged two-electron ions, the most interesting levels are all in the $n = 2$ shell. However, there are more of these than in the H-like ions, because electron–electron interaction and correlation come into play. There are singlet and triplet levels, and spin–changing E1 and M2 intercombination transitions connecting the two term systems (Fig. 3). Some of the weak transition branches have recently been driven by lasers acting on fast N^{5+} ion beams, establishing very precise connections of singlet and triplet terms [87,88]. The $1s2p\ ^3P_1^0$ level mixes with the $1s2p\ ^1P_1^0$ singlet level and thus decays to the singlet ground state (the Z^{10} scaling of the transition probability (same scaling, but for other reasons than for the M1 transition above) makes this the dominant decay branch beyond nitrogen ($Z = 7$), and the fine structure transition hardly observable beyond $Z = 12$ [89]. The $1s2p\ ^3P_2^0$ level has the fine structure transition to the $1s2s\ ^3S_1$ level and a magnetic quadrupole (M2) decay branch to the ground level; the M2 transitions scale with Z^8 and exceeds the

competitor beyond Ar ($Z = 18$). Now, the $1s2p\ ^3P_0^0$ level is the lowest ^3P level above the $1s^2\ ^1S_0$ ground state, and it also has $J = 0$, which strictly forbids single photon transitions to take place. Multiphoton transition rates have been calculated, but found to be extremely low. However, if the nucleus has a spin I, hyperfine interaction splits the fine structure levels. There then are hyperfine levels of the $J = 0$ and $J = 1$ levels that have the same total quantum number F from the coupling of J and I, and therefore they mix. Hyperfine interaction mixes $1s2p\ ^3P_0^0$ and $1s2p\ ^3P_1^0$, and spin–orbit interaction mixes $1s2p\ ^3P_1^0$ and $1s2p\ ^1P_1^0$, and in this roundabout way, the $J = 0$ level can decay by emission of a single photon to ground, albeit with low probability. All the mixings depend—among other contributions—on the level separation. Where the level separation is known, one learns about the mixing operator from a lifetime measurement. Vice versa, a beam–foil lifetime measurement on Ag^{45+}, assuming theoretical understanding of the mixing process, can tell the level separation which may be difficult to obtain experimentally [48].

The allowed transitions within the $n = 2$ shell have been exploited for Lamb shift measurements, because spin–conservation hinders the fast decay to the ground state and thus prevents the corresponding level broadening, at the cost of having to deal with a more complex system. Much work on these has been done by beam-foil spectroscopy over the years, and surveys and details can easily be found elsewhere [7]. However, there also is a peculiar decay that is still of active research interest, that is the transition $1s^2\ ^1S_0$–$1s2s\ ^3S_1$. This decay had been declared by theoreticians to proceed via multiphoton processes only [90], but was then identified as a single-photon magnetic dipole (M1) line in the sun [91]. The transition is purely caused by relativistic effects, and the transition probability A_{M1} scales with Z^{10}. Apparently the most precise calculation for a wide range of elements at present is that by Johnson et al. [92]. This transition rate has been measured for atoms and ions from neutral He to Xe^{52+}, with lifetimes from thousands of seconds to picoseconds, spanning 15 orders of magnitude. The techniques reached from laser absorption and ion traps for He and Li^+ via dielectronic recombination at a storage ring [93], EBIT [94–99], a (relatively) slow recoil ion beam [100] to beam–foil spectroscopy [38,39]. In the extreme, at $Z = 92$, the $1s2s\ ^3S_1$ lifetime is much shorter than that of the $1s2p\ ^3P_0^0$ level which repopulates the upper level. [The decay of the $1s2p\ ^3P_0^0$ level to the $1s2s\ ^3S_1$ level is the only one of these fine structure transitions to survive up to high Z (in isotopes without hyperfine structure), the others have so much stronger decay branches to the ground state that practically nothing is seen of the transition within the same shell.] This cascade in the $1s2s\ ^3S_1$ level decay curve has been evaluated in order to derive a measure of the $n = 2$ Lamb shift in He-like uranium [13] from the $^3P_0^0$ level lifetime, which depends on the $^3S_1$–$^3P_0^0$ level splitting of which the Lamb shift is a sizable fraction.

Because nowadays He-like ions can also be calculated with high precision, precision lifetime numbers on the $1s2s\ ^3S_1$ level are of interest in order to test these calculations. Calculated lifetimes depend on details of the atomic wave functions where wavelength measurements are less sensitive. Thus both types of experiments are wanted. The first very precise lifetime measurements in this case used an electron cooler at a heavy ion storage ring: A beam of electrons of low relative energy is merged with the ion beam. If the total energy is degenerate with a doubly excited state, radiative stabilization may happen and an electron may be captured. As two electrons are involved, this is termed dielectronic recombination (DR). There are resonances, so that individual levels can be studied, and the change of charge state can be detected with high efficiency. The reaction rates are low, so that the stored ion beam is only minimally perturbed by this DR process. Thus the DR process can be used as an almost nonintrusive probe for the remaining population of a particular excited state, if the neighbouring states are far enough away so that the resonances can be separated. This technique has been demonstrated with remarkably precise results at the Heidelberg TSR ring, measuring the lifetime of the lowest triplet level, $1s2s\ ^3S_1$, in He-like ions of C and N. The results are $\tau = (20.62 \pm 0.09)$ ms for

C^{4+} and $\tau = (3.91 \pm 0.07)$ ms for N^{5+} [93]. Meanwhile there have also been measurements at EBIT on such ions, from N^{5+} to about S^{14+}. The most precise of these so far was the measurement on O^{6+} ($\pm 0.5\%$) [98] and Ne^{8+} [99]. In the early EBIT measurements [94], the electron beam energy was raised above the excitation threshold for the wanted level and then lowered, and the wanted signal derived from the difference. In the newer measurements, the electron beam is switched off completely, and then EBIT runs as a Penning trap with confinement times of many seconds [95,96]. The more recent results on this particular transition all are in agreement with theory [92]. Various calculations, however, do differ at the 1% level (and show different Z-dependences). Now the interest is to have experiment gain so much in precision that it can discriminate even among such precise calculations.

The $2s\ ^2S_{1/2}$ level in H-like ions can decay either by two-photon emission or by M1 decay. For the $1s2s\ ^1S_0$ level in He-like ions, there only is a two-photon decay. The two-photon energy spectrum is a continuum, as only the sum energy of the two photons is specified (the total transition energy). In beam–foil spectra, the continua of H- and He-like origin overlap, and it is very difficult to disentangle them in order to study the spectral shapes (which tell about interferences of the atomic processes) [36]. With a heavy-ion storage ring, storing only a single charge state, this is easier. However, in order to see light, there first has to be excitation, and the lifetimes involved are too short to separate excitation and detection. The excitation can be initiated by passing the ions through a dilute gas target. This implies that a higher charge state has been stored before, naked or one-electron ions. Single electron capture is more likely than double electron capture, and the capture processes also depend on the collision energy. An experiment in this context used the ESR storage ring at GSI to prepare the ions and provide them at specific energies in a wide range [101]. The ions were then slowly extracted, so that electronic pile-up could be avoided. A variety of x-ray detectors was employed to study the two photons of interest in coincidence, as well as other clues to the capture processes.

11. Li-like ions

Three-electron ions, with a single electron outside of a closed shell, are not quite as precisely calculable as true one-electron ions, but are quite competitive in practice. Also, the closed $n = 1$ shell means that the decays are restricted to smaller term differences which then reveal more detail. Measurements with fast ion beams [14,40] and EBIT [58] reach up to U^{89+} and, because of the better experimental handling, may be even more precise in terms of the QED contributions than those on the true one-electron systems.

12. Be-like ions

Four-electron ions are closely related to the He-like two-electron-ions discussed above. The *K* shell, however, is filled, and thus the x-ray decay not available. The resonance and intercombination transitions for most ions of the sequence are then in the UV and EUV. This renders all other transitions, in particular the transitions between fine structure levels, better observable, as the competitor is absent. Also, for the low-lying levels, the two electrons are in the same shell, interacting more strongly with each other than in He-like ions with one electron in the $n = 1$ shell. Otherwise, of course, there are extensive similarities (Fig. 4).

C^{2+} may serve as a numerical example. Carbon is an element not only abundant on Earth, but also in the Sun and other stars and cosmic plasmas. Beyond the stable (singlet) ground state, $2s^2\ ^1S_0$ in spectroscopic notation, Be-like ions have a few long-lived levels, the lowest ones in the triplet system. The lowest of these, $2s2p\ ^3P_0^0$, is truly long-lived, because no single photon can combine this level with the only lower level, the ground state. For C^{2+}, theory tells of 10^8 s or more than 3 years [102], a lifetime that seems beyond laboratory measurements by far. In order to

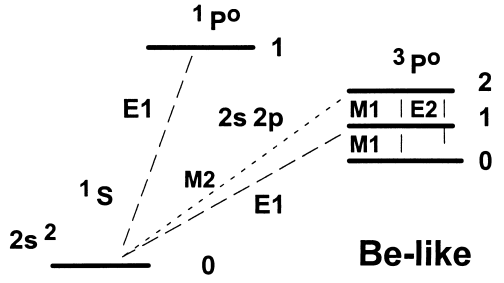

Fig. 4. Level scheme of the lowest $n = 2$ levels of a four-electron ion, with the dominant transitions indicated. (The energy intervals are not to scale.)

measure this, one would need to have a vacuum with collisions that are even rarer, and much of outer space has more matter than would be permissible for this.

There are two more levels in the same level multiplet or term, $2s2p\ ^3P_1^0$ and $2s2p\ ^3P_2^0$. The first of these can decay to the ground state if the spin changes, a serious obstacle. Instead of the fraction-of-a-nanosecond—lifetime of the related singlet (resonance) level, theory indicates a lifetime of about 10 ms—about 8 orders of magnitude more! This lifetime has recently been measured at a heavy-ion storage ring [103]: Negative carbon ions from an ion source were accelerated to an energy of 1.5 MeV, sent through a gas where some of them lost three electrons to become C^{2+} ions. These were further accelerated to about 4.5 MeV (a peculiarity of the tandem accelerator used here), separated from other charge state and energy ions in a magnetic field, guided (by further magnetic and electric fields) to a storage ring (Fig. 5), and inserted into the guiding fields there, all under very good vacuum. The ion beam was accumulated over about 30 turns in the ring. Then the injection was stopped and the beam left to itself, but observed by particle and photon detectors and current-measuring devices. All excitation had to happen in the stripping process in the accelerator, because there was no later interaction of ions and matter. (In this sense, this was a beam–gas experiment in the beam–foil tradition.) The transport to the storage ring and the injection process took about 1 ms. This is short compared to the lifetime of interest, so most of the ions excited to the level of interest would still be excited after that time.

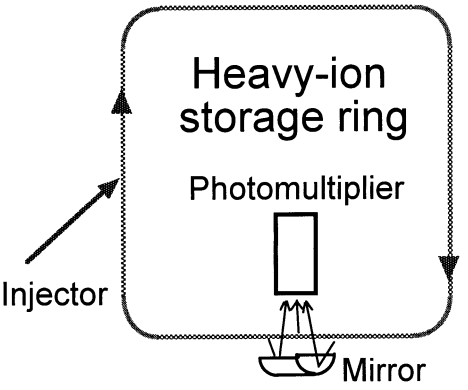

Fig. 5. Optical detection of the decays of long-lived atomic levels in an ion storage ring.

However, the vast majority of other levels has lifetimes in the nanosecond to microsecond range and would have decayed to low-lying levels long before observation began. Observation of the decay signal (Fig. 6) of the level of interest proceeded as time-resolved observation of the 190 nm light from the intercombination decay to the ground state, by a low-noise photomultiplier aided by a simple light collection system, viewing a section of about 5 cm, that is about 10^{-3} of the 55.4 m circumference of the TSR heavy-ion storage ring. After 200 ms (much longer than the lifetime of interest) the stored ion

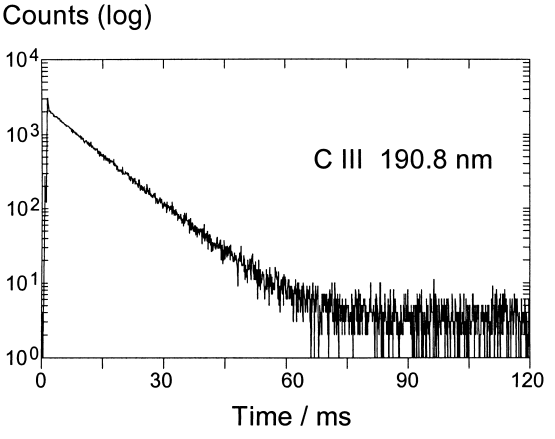

Fig. 6. Sample curve of an experiment on doubly charged carbon ions [103]. The range shown includes the filling of the storage ring (early times) and the decrease of the optical signal until it disappears into the detector background.

beam was dumped, and the storage ring refilled. The ion storage time constant was about 10 s, so that the corresponding correction to the optical signal was as small as 0.1%. The beauty and cleanliness of this experiment resulted from several factors: ion production and selection occurred in a place different from the storage and observation, and by storage at mega-electron volt energies at which collision cross sections are small and a direct monitoring is possible, the measurement reached an extremely small uncertainty of only 0.13%. This meant a factor of 50 improvement (and a notable correction) over earlier measurements with a radiofrequency ion trap.

For those near-neutral ions, theory has problems. The Coulomb field of the nucleus is not so much stronger than the influences of the other electrons, and electron-electron correlation effects are important. Atomic structure there has the benefit of a guide, the Ritz principle, for the optimization of the lowest level of each symmetry: A computational imperfection will yield a level value higher than the true one—the lowest from a number of trials is assumed to be best. However, the calculation of transition probabilities involves the square of the radial wave functions, which may be nonorthogonal and for which there is no such optimization rule. One may assume that perfect wave functions will describe the ion perfectly, but experiment tests whether in fact theory is close to that required perfection.

For the ions of the Be isoelectronic sequence, a single set of calculations now is available that appears to represent the lifetime trends of both the $2s2p\ ^1P_1^0$ resonance level and of the intercombination decay of the $2s2p\ ^3P_1^0$ level discussed above [104]. For the singlet transition, theory is more precise than experiment, whereas for the intercombination transition—after years of lacking any good data—experiment is more precise now than even the best calculation. The situation seems much less well understood for ions with the same number of electrons in the outermost open (valence) shell, but more inner closed shells, like the Mg isoelectronic sequence (see the following).

In C^{2+}, the higher-lying other fine structure level, $2s2p\ ^3P_2^0$, predominantly decays via a magnetic quadrupole decay to the ground state. It would be good to also know the $2s2p\ ^3P_2^0$ level lifetime precisely, which calculation puts near 180 s. Such a long lifetime is a challenge for experiment. In more highly charged ions of the Be sequence, the M1 decay to the $2s2p\ ^3P_1^0$ level dominates. In contrast, it ought to be possible to measure the (just less than 1 ms) lifetime of the same $2s2p\ ^3P_2^0$ level in, say, Ti^{18+}, using the very same equipment as for the above mentioned experiment on C^{2+}, and obtain a decay rate that is largely given by the M1 transition amplitude.

A number of forbidden transition rates ("forbidden" means not possible by electric–dipole transition, because of parity and J values involved) in few-electron ions have been measured by now. Among these are M1/E2 transitions in Si^{6+} and Si^{8+}, which are of interest in the diagnostics of astrophysical plasmas [105]. The first EBIT lifetime measurements on such forbidden transitions in Ar^{13+}, Kr^{22+}, and Xe^{32+} [106–109] have shown the principle to work well, but have not yet reached a precision of better than 5%. Part of the problem is that photomultipliers for visible light are noisier than x-ray detectors (where more energy per photon makes it easier to discriminate against unwanted signals). Also, a spectrometer has a much lower detection efficiency (by solid angle and detector response) than an x-ray diode. However, the 1% uncertainty range seems in reach at EBIT even with visible forbidden lines. A further help in this quest is provided by an electron beam energy that can be set to fairly low values (below 1 keV), so that individual charge states can be discriminated against. EBIT has not only reached U^{91+} [9], but can produce spectra of the full range of few-electron ions of uranium [58]. This offers systematic access to wavelength data that are sensitive to QED effects, and the quality of the theoretical treatment is found to be different in the various ions. Also, EBIT with its low-density environment is able to show forbidden lines that are collisionally quenched in most other light sources. An example is the $3d^4\ ^5D_2$–$^5D_3$ transition in Ti-like ions, that has been found (by theoretical studies [110]) to vary very little in wavelength for a wide range of ion charges (the normal case is a Z^4 variation of such fine structure intervals—very

steep [111–113])! The wavelength is in the near ultraviolet range, very handy for the diagnostics of future hot low-density plasmas like envisaged for large fusion test devices. Guided by theory, this line has subsequently been seen in four different EBITs [108,114,115], in ions up to Au^{57+} [109], and its transition rate been measured in Xe^{32+} [106]. EBIT seems a very useful light source to study a multitude of those forbidden transitions and establish their systematics, so that they then can be used in the diagnostics of whatever plasmas.

For some atomic spectroscopy problems, there will be competition of heavy-ion storage rings and EBIT. For example, the same hyperfine-interaction induced decay process as discussed with He-like ions is possible with Be-like (and Mg-like etc.) ions, too [116,117]. Because the resonance transition has a lower transition rate in Be-like ions, the intercombination and hyperfine-induced transitions will be correspondingly slower, too. For the Be sequence ($n = 2$ levels) and the closely related Mg sequence ($n = 3$ levels) this means (roughly) millisecond lifetimes of the $J = 0$ level, for ions up to uranium. In principle this can be done by using either ion storage rings or EBIT. However, to produce such highly charged ions for a storage ring requires a source for extremely high charge states (EBIT's sister EBIS?) or an accelerator system in first place—and therefore it would be much more sensible, though perhaps not quite so precise a result, to use EBIT all the way. For lower charge states, heavy-ion storage rings might do better, because of their cleaner physical conditions.

13. Mg I sequence

The intercombination decay of the $3s3p\ ^3P_1^0$ level in Mg-like ions has been studied by ion trap work for Al^+ and Si^{2+} (the latter also by a pilot heavy-ion storage ring experiment [118]), and by beam–foil spectroscopy for a number of ions from Fe onwards [15,119]. Although there is reasonable agreement (small error bars for very few ions only) up to about $Z = 35$, the data beyond either show an unexplained deviation from standard calculations or are not particularly precise. More and better data are needed, and similarly so for the Al I [120] and Si I isoelectronic sequences, with three or four electrons in an open shell. The same holds for the next higher shells, that is the Zn I, Ga I and Ge I sequences: Experimental wavelength data are grossly incomplete, and reliable (in need of semiempirical adjustment and not necessarily accurate even then) calculations rare and incomplete. The experimental lifetime data on the intercombination decays are good enough to oust some calculations. However, neither experiment nor theory are up to detailed tests yet.

14. Interactions with atoms or electrons in the storage ring

In addition to the classical spectroscopy that depends on the excitation of ions from the ground state, there are other intriguing types of spectroscopy that "comes from above:" Radiative recombination (RR) and laser-induced recombination. Both are arranged for to happen inside the electron cooler of an ion storage ring. If ions and electrons travel alongside at the same speed, recombination occurs as a two-body process, and it populates the target ion from above. The ion beam is deflected by the dipole magnets of the storage ring before it reaches the detector. If electron capture took place, the ion trajectories of unharmed and recombined ions separate in the field of the dipole magnet. A coincidence of the ion with a photon from the RR process will contribute to a very clean spectrum. In this way, X-ray spectra of one-electron Au^{78+} ions have been obtained [84,85] which are among the most sensitive in terms of QED contributions.

The recombination process can be enhanced by offering the photon field of a laser beam [121,122], so that a transition from the continuum to a selected atomic shell is possible, and further selected transitions from there. Observation along the ion beam suffers from maximum Doppler shift (may be helpful for using a technically good laser on an otherwise difficult to reach transition) but minimum broadening (good for high-resolution spectroscopy). This tech-

nique permits the selected population of high-lying levels in multicharged ions without the need to first overcome the large energy steps from the ground state to even the lowest excited levels. Obviously, photon spectroscopy is not yet at the end of its many possibilities.

References

[1] B. Edlén, F. Tyrén, Nature 143 (1939) 940.
[2] B. Edlén, Z. Astrophys. 22 (1942) 30.
[3] M.A. Levine, R.E. Marrs, J.R. Henderson, D.A. Knapp, M.B. Schneider, Phys. Scr. T 22 (1988) 157.
[4] L. Kay, Phys. Lett. 5 (1963) 36.
[5] S. Bashkin, A.B. Meinel, Astrophys. J. 139 (1964) 413.
[6] S. Bashkin, Science 148 (1965) 1047.
[7] E. Träbert, in Accelerator-based Atomic Physics—Techniques and Applications, S.M. Shafroth, J.C. Austin (Eds.), AIP, Woodbury, NY, 1997, p. 567.
[8] H. Gould, D. Greiner, P. Lindstrom, T.J.M. Symons, H. Crawford, Bull. Am. Phys. Soc. 28 (1983) 1345.
[9] R.E. Marrs, S.R. Elliott, D.A. Knapp, Phys. Rev. Lett. 72 (1994) 4082.
[10] E. Hylleraas, Z. Phys. 54 (1929) 347; 65 (1930) 209.
[11] B. Edlén, Atomic Spectra, in Handbuch der Physik Vol. XXVII S. Flügge (Ed.), Springer, Heidelberg, 1964.
[12] P.H. Heckmann, E. Träbert, Introduction to the Spectroscopy of Atoms, North-Holland, Amsterdam, 1989.
[13] C.T. Munger, H. Gould, Phys. Rev. Lett. 57 (1986) 2927.
[14] J. Schweppe, A. Belkacem, L. Blumenfeld, N. Claytor, B. Feinberg, H. Gould, V. Kostroun, L. Levy, S. Misawa, R. Mowat, M. Prior, Phys. Rev. Lett. 66 (1991) 1434.
[15] E. Träbert, J. Doerfert, J. Granzow, R. Büttner, U. Staude, K.-H. Schartner, P. Rymuza, L. Engström, R. Hutton, Z. Phys. D 32 (1994) 295.
[16] D.G. Ellis, I. Martinson, E. Träbert, Comm. At. Mol. Phys. 22 (1989) 241.
[17] E. Träbert, Phys. Scr. 48 (1993) 699.
[18] P. Beiersdorfer, A.L. Osterheld, J. Scofield, B. Wargelin, R.E. Marrs, Phys. Rev. Lett. 67 (1991) 2272.
[19] K.P. Dere, E. Laudi, H.E. Mason, B.C. Monsignori Fossi, P.R. Young, Astron. Astrophys. 125 (1997) 149.
[20] C. Jupén, R.C. Isler, E. Träbert, Mon. Not. R. Astron. Soc. 264 (1993) 627.
[21] N.J. Peacock, M.F. Stamp, J.D. Silver, Phys. Scr. T 8 (1984) 10.
[22] B. Denne, E. Hinnov, Phys. Scr. 35 (1987) 811.
[23] P. Beiersdorfer, S. von Goeler, M. Bitter, E. Hinnov, K. Bell, S. Bernabei, J. Felt, K.W. Hill, R. Hulse, J. Stevens, S. Suckewer, J. Timberlake, A. Wouters, M.H. Chen, J.H. Scofield, D.D. Dietrich, M. Gerassimenko, E. Silver, R.S. Walling, P. Hagelstein, Phys. Rev. A 37 (1988) 4153.
[24] B. Denne, E. Hinnov, J. Ramette, B. Saoutic, Phys. Rev. A 40 (1989) 1488.
[25] J. Sugar, V. Kaufman, D.H. Baik, Y.-K. Kim, J. Opt. Soc. Am. B 8 (1991) 1975.
[26] J. Reader, V. Kaufman, J. Sugar, J.O. Ekberg, U. Feldman, C.M. Brown, J.F. Seely, W.L. Rowan, J. Opt. Soc. Am. B 4 (1987) 1821.
[27] J.F. Seely, R.A. Wagner, Phys. Rev. A 41 (1990) 5246.
[28] J.O. Ekberg, U. Feldman, J.F. Seely, C.M. Brown, Phys. Scr. 40 (1989) 643.
[29] J.O. Ekberg, U. Feldman, J.F. Seely, C.M. Brown, B.J. MacGowan, D.R. Kania, C.J. Keane, Phys. Scr. 43 (1991) 19.
[30] U. Feldman, J.O. Ekberg, J.F. Seely, C.M. Brown, D.R. Kania, B.J. MacGowan, C.J. Keane, W.E. Behring, J. Opt. Soc. Am. B 8 (1991) 531.
[31] D.R. Kania, B.J. MacGowan, C.J. Keane, C.M. Brown, J.O. Ekberg, J.F. Seely, U. Feldman, J. Opt. Soc. Am. B 7 (1990) 1993.
[32] J. Reader, N. Acquista, J. Opt. Soc. Am. B 9 (1992) 347.
[33] J. Nilsen, J.H. Scofield, Phys. Scr. 49 (1994) 588.
[34] E. Träbert, P.H. Heckmann, R. Hutton, I. Martinson, J. Opt. Soc. Am. B 5 (1988) 2173.
[35] H.G. Berry, R.W. Dunford, A.E. Livingston, Phys. Rev. A 47 (1993) 698.
[36] R.W. Dunford, H.G. Berry, D.A. Church, M. Hass, C.J. Liu, M.L.A. Raphaelian, L.J. Curtis, A.E. Livingston, Phys. Rev. A 48 (1993) 2729.
[37] R.W. Dunford, H.G. Berry, S. Cheng, E.P. Kanter, C. Kurtz, B.J. Zabransky, A.E. Livingston, L.J. Curtis, Phys. Rev. A 48 (1993) 1929.
[38] A. Simionovici, B.B. Birkett, R. Marrus, P. Charles, P. Indelicato, D.D. Dietrich, K. Finlayson, Phys. Rev. A 49 (1994) 3553.
[39] S. Cheng, R.W. Dunford, C.J. Liu, B.J. Zabransky, A.E. Livingston, L.J. Curtis, Phys. Rev. A 49 (1994) 2347.
[40] R. Büttner, U. Staude, M. Nicolai, J. Brauckhoff, K.-H. Schartner, F. Folkmann, P.H. Mokler, Nucl. Instrum. Methods Phys. Res. B 98 (1995) 41.
[41] E. Träbert, Mon. Not. R. Astron. Soc. 297 (1998) 399.
[42] J.A. Leavitt, J.W. Robson, J.O. Stoner Jr., Nucl. Instrum. Methods 110 (1973) 435.
[43] K.-E. Bergkvist, J. Opt. Soc. Am. 66 (1976) 837.
[44] E. Träbert, J. Doerfert, J. Granzow, R. Büttner, J. Brauckhoff, M. Nicolai, K.-H. Schartner, F. Folkmann, P.H. Mokler, Phys. Lett. A 202 (1995) 91.
[45] I. Kink, R. Hutton, B. Nyström, I. Martinson, K. Ishii, K. Ando, T. Kambara, Y. Nakai, T.M. Kojima, Y. Awaya, Phys. Rev. A 55 (1997) 3229.
[46] E. Träbert, Nucl. Instrum. Methods Phys. Res. B 23 (1987) 287.
[47] L. Engström, C. Jupén, B. Denne, S. Huldt, W.T. Meng, P. Kaijser, U. Litzén, I. Martinson, J. Phys. B 13 (1980) L143.
[48] B.B. Birkett, J.-P. Briand, P. Charles, D.D. Dietrich, K. Finlayson, P. Indelicato, D. Liesen, R. Marrus, A. Simionovici, Phys. Rev. A 47 (1993) R2454.
[49] M. Cornille, T. LuDac, D. Hitz, S. Bliman, G.A. Heckman, E.J. Knystautas, Phys. Rev. A 43 (1991) 115.
[50] P. Boduch, M. Chantepie, D. Hennecart, X. Husson, D. Lecler, M. Druetta, M. Wilson, Phys. Scr. 46 (1992) 337.

[51] D.A. Church, M. Druetta, R. Dunford, C.-J. Lin, C. Froese Fischer, I. Idrees, V.M. Umar, J. Opt. Soc. Am. B 9 (1992) 2159.
[52] R. Hutton, S. Huldt, B. Nyström, F. Heijkenskjöld, P. Glans, M.O. Larsson, Phys. Scr. 48 (1993) 569.
[53] H. Cederquist, C. Biedermann, N. Selberg, L. Liljeby, E. Beebe, Phys. Scr. T 46 (1993) 218.
[54] P. van Kampen, R. Hallin, F. Heijkenskjöld, A. Langereis, M.O. Larsson, C. Nordling, B. Nyström, G. O'Sullivan, A. Wännström, Phys. Scr. 49 (1994) 198.
[55] J.-Y. Chesnel, H. Merabet, F. Frémont, G. Cremer, X. Husson, D. Lecler, G. Rieger, A. Spieler, M. Grether, N. Stolterfoht, Phys. Rev. A 53 (1996) 4198.
[56] J. Bernard, L. Chen, A. Denis, J. Désesquelles, S. Martin, Phys. Scr. 56 (1997) 26.
[57] T.E. Cowan, C.L. Bennett, D.D. Dietrich, J. Bixler, C.J. Hailey, C.J. Henderson, D.A. Knapp, M.A. Levine, R.E. Marrs, M.B. Schneider, Phys. Rev. Lett. 66 (1991) 1150.
[58] P. Beiersdorfer, D. Knapp, R.E. Marrs, S.R. Elliott, M.H. Chen, Phys. Rev. Lett. 71 (1993) 3939.
[59] J.D. Gillaspy, Phys. Scr. T 65 (1996) 168.
[60] K. Widmann, P. Beiersdorfer, V. Decaux, M. Bitter, Phys. Rev. A 53 (1996) 2200.
[61] J. Crespo López-Urrutia, P. Beiersdorfer, D.W. Savin, K. Widmann, Phys. Rev. Lett. 77 (1996) 826.
[62] S.R. Elliott, P. Beiersdorfer, M.H. Chen, V. Decaux, D.A. Knapp, Phys. Rev. C 57 (1998).
[63] J.R. Crespo López-Urrutia, P. Beiersdorfer, K. Widmann, B.B. Birkett, A.-M. Mårtensson-Pendrill, M.G.H. Gustavsson, Phys. Rev. A 57 (1998) 879.
[64] P. Beiersdorfer, A.L. Osterheld, V. Decaux, K. Widmann, Phys. Rev. Lett. 77 (1996) 5353.
[65] R.O. Sayer, Rev. Phys. Appl. 12 (1977) 1543.
[66] K. Shima, N. Kuno, M. Yamanouchi, H. Tawara, At. Data Nucl. Data Tables 51 (1992) 173.
[67] F.M. Penning, Physica 3 (1936) 873.
[68] W. Paul, H. Steinwedel, Z. Naturforsch. A 8 (1953) 448.
[69] K.H. Kingdon, Phys. Rev. 21 (1923) 408.
[70] A.G. Calamai, C.E. Johnson, Phys. Rev. A 42 (1990) 5425.
[71] L. Yang, D.A. Church, S. Tu, J. Jin, Phys. Rev. A 50 (1994) 177.
[72] D.P. Moehs, D.A. Church, Phys. Rev. A 58 (1998) 1111.
[73] Proceedings of the Nobel Symposium 91, I. Bergström, C. Carlberg, R. Schuch (Eds.), Physica Scr. T 59 (1995).
[74] Atomic Physics and Stored Highly Charged Ions, A. Wolf, H.-J. Kluge, H. Orth (Eds.), Baltzer, Amsterdam 1996/Hyp. Int., 99 (1996).
[75] A. Müller, A. Wolf, in Accelerator-based Atomic Physics—Techniques and Applications, S.M. Shafroth, J.C. Austin (Eds.), AIP Press, Woodbury, NY, 1997, p. 147.
[76] Th. Stöhlker, Phys. Scr. T 73 (1997) 29.
[77] P.H. Mokler, Th. Stöhlker, C. Kozhuharov, R. Moshammer, P. Rymuza, F. Bosch, T. Kandler, Phys. Scr. T 51 (1994) 28.
[78] W.R. Johnson, G. Soff, At. Data Nucl. Data Tables 33 (1985) 405.
[79] P. v. Brentano, D. Platte, D. Budelsky, L. Kremer, H.J. Pross, F. Scheuer, Phys. Scr. T 46 (1993) 162.
[80] C.Y. Fan, M. Garcia-Munoz, I.A. Sellin, Phys. Rev. 161 (1967) 6.
[81] H. Gould, R. Marrus, Phys. Rev. A 28 (1983) 2001.
[82] E. Träbert, in The Spectrum of Atomic Hydrogen: Advances, G.W. Series (Ed.), World Scientific, Singapore, 1988, p. 332.
[83] G. Hölzer, E. Förster, D. Klöpfel, P. Beiersdorfer, G.V. Brown, J. Crespo López-Urrutia, K. Widmann, Phys. Rev. A 57 (1998) 945.
[84] H.F. Beyer, D. Liesen, F. Bosch, K.D. Finlayson, M. Jung, O. Klepper, R. Moshammer, K. Beckert, H. Eickhoff, B. Franzke, F. Nolden, P. Spädtke, M. Steck, Phys. Lett. A 184 (1994) 435.
[85] D. Liesen, H.F. Beyer, K.D. Finlayson, F. Bosch, M. Jung, O. Klepper, R. Moshammer, K. Beckert, H. Eickhoff, B. Franzke, F. Nolden, P. Spädtke, M. Steck, G. Menzel, R.D. Deslattes, Z. Phys. D 30 (1994) 307.
[86] I. Klaft, S. Borneis, T. Engel, B. Fricke, R. Grieser, G. Huber, T. Kühl, D. Marx, R. Neumann, S. Schröder, P. Seelig, L. Völker, Phys. Rev. Lett. 73 (1994) 2425.
[87] E.G. Myers, D.J.H. Howie, J.K. Thompson, J.D. Silver, Phys. Rev. Lett. 76 (1996) 4899.
[88] J.K. Thompson, D.J.H. Howie, E.G. Myers, Phys. Rev. A 57 (1998) 180.
[89] H.A. Klein, F. Moscatelli, E.G. Myers, E.H. Pinnington, J.D. Silver, E. Träbert, J. Phys. B 18 (1985) 1483.
[90] G. Breit, E. Teller, Astroph. J. 91 (1940) 215.
[91] A.H. Gabriel, C. Jordan, Nature 221 (1969) 947.
[92] W.R. Johnson, D.R. Plante, J. Sapirstein, in Advances of Atomic, Molecular and Optical Physics, Vol. 35, B. Bederson, H. Walther (Eds.), Academic, San Diego, 1995, p. 255.
[93] H.T. Schmidt, P. Forck, M. Grieser, D. Habs, J. Kenntner, G. Miersch, R. Repnow, U. Schramm, T. Schüssler, D. Schwalm, A. Wolf, Phys. Rev. Lett. 72 (1994) 1616.
[94] B.J. Wargelin, P. Beiersdorfer, S.M. Kahn, Phys. Rev. Lett. 71 (1993) 2196.
[95] P. Beiersdorfer, L. Schweikhard, J. Crespo López-Urrutia, K. Widmann, Rev. Sci. Instrum. 67 (1996) 3818.
[96] P. Beiersdorfer, B. Beck, St. Becker, L. Schweikhard, Int. J. Mass Spectrom. Ion Processes 157/158 (1996) 149.
[97] G.S. Stefanelli, P. Beiersdorfer, V. Decaux, K. Widmann, Phys. Rev. A 52 (1995) 3651.
[98] J.R. Crespo López-Urrutia, P. Beiersdorfer, D.W. Savin, K. Widmann, Phys. Rev. A 58 (1998) 238.
[99] E. Träbert, P. Beiersdorfer, G.V. Brown, A.J. Smith, S.B. Utter, M.F. Gu, D.W. Savin, Phys. Rev. A, in press.
[100] G. Hubricht, E. Träbert, Z. Phys. D 7 (1987) 243.
[101] P.H. Mokler, Th. Stöhlker, R.W. Dunford, A. Gallus, T. Kandler, G. Menzel, H.-T. Prinz, P. Rymuza, Z. Stachura, P. Swiat, A. Warczak, Z. Phys. D 35 (1995) 77.
[102] C. Laughlin, Phys. Lett. 75A (1980) 199.
[103] J. Doerfert, E. Träbert, A. Wolf, D. Schwalm, O. Uwira, Phys. Rev. Lett. 78 (1997) 4355.
[104] P. Jönsson, C. Froese Fischer, E. Träbert, J. Phys. B 31 (1998) 3497.
[105] E. Träbert, A. Wolf, E.H. Pinnington, J. Linkemann, E.J. Knystautas, A. Curtis, N. Bhattacharya, H.G. Berry, Can. J. Phys. in press.

[106] F.G. Serpa, C.A. Morgan, E.S. Meyer, J.D. Gillaspy, E. Träbert, D.A. Church, E. Takács, Phys. Rev. A 55 (1997) 4196.
[107] F.G. Serpa, J.D. Gillaspy, E. Träbert, J. Phys. B 31 (1998) 3455.
[108] F.G. Serpa, E.W. Bell, E.S. Meyer, J.D. Gillaspy, J.R. Roberts, Phys. Rev. A 55 (1997) 1832.
[109] E. Träbert, P. Beiersdorfer, S.B. Utter, J.R. Crespo López-Urrutia, Phys. Scr. 58 (1998) 599.
[110] U. Feldman, P. Indelicato, J. Sugar, J. Opt. Soc. Am. B 8 (1991) 3.
[111] B. Edlén, Phys. Scr. T 3 (1983) 5.
[112] B. Edlén, Phys. Scr. T 8 (1984) 5.
[113] V. Kaufman, J. Sugar, J. Phys. Chem. Ref. Data 15 (1986) 321.
[114] F.G. Serpa, E.S. Meyer, C.A. Morgan, J.D. Gillaspy, J. Sugar, J.R. Roberts, C.M. Brown, U. Feldman, Phys. Rev. A 53 (1996) 2220.
[115] D.J. Bieber, H.S. Margolis, P.K. Oxley, J.D. Silver, Phys. Scr. T 73 (1997) 64.
[116] J.P. Marques, F. Parente, P. Indelicato, Phys. Rev. A 47 (1993) 929.
[117] J.P. Marques, F. Parente, P. Indelicato, At. Data Nucl. Data Tables 55 (1993) 157.
[118] E. Träbert, J. Linkemann, A. Wolf, X. Tordoir, J. Phys. B 32 (1999) 537.
[119] R. Hutton, Phys. Scr. T 73 (1997) 25.
[120] E. Träbert, U. Staude, P. Bosselmann, K.H. Schartner, P.H. Mokler, X. Tordoir, Eur. Phys. J. D 2 (1998) 117.
[121] S. Borneis, F. Bosch, T. Engel, M. Jung, I. Klaft, O. Klepper, T. Kühl, D. Marx, R. Moshammer, R. Neumann, S. Schröder, P. Seelig, L. Völker, Phys. Rev. Lett. 72 (1993) 207.
[122] T. Schüssler, U. Schramm, T. Rüter, C. Broude, M. Grieser, D. Habs, D. Schwalm, A. Wolf, Phys. Rev. Lett. 75 (1995) 802.